Title

1,25-dihydroxyvitamin D3-eluting nanofibrous dressings induce endogenous antimicrobial peptide expression

Journal

Nanomedicine, 13(12)

ISSN

1743-5889

Authors

Jiang, Jiang
Zhang, Yang
Indra, Arup K
et al.

Publication Date

2018-06-01

DOI

10.2217/nnm-2018-0011

Peer reviewed

Research Article

For reprint orders, please contact: reprints@futuremedicine.com

Nanomedicine

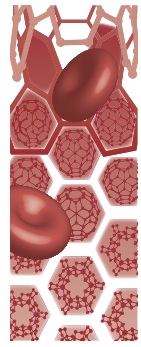

1α,25-dihydroxyvitamin D_3-eluting nanofibrous dressings induce endogenous antimicrobial peptide expression

Jiang Jiang[1], Yang Zhang[2,3], Arup K Indra[2,4,5,6], Gitali Ganguli-Indra[4,6], Mai N Le[4], Hongjun Wang[1], Ronald R Hollins[7], Debra A Reilly[7], Mark A Carlson[8,9], Richard L Gallo[10], Adrian F Gombart**[2,3] & Jingwei Xie*[,1]

[1]Department of Surgery, Transplant & Holland Regenerative Medicine Program, University of Nebraska Medical Center, Omaha, NE 68198, USA

[2]Department of Biochemistry & Biophysics, Linus Pauling Institute, Oregon State University, Corvallis, OR 97331, USA

[3]Nutrition Graduate Program, School of Biological & Population Health Sciences, College of Public Health & Human Sciences, Oregon State University, Corvallis, OR 97331, USA

[4]Department of Pharmaceutical Sciences, College of Pharmacy, Oregon State University, Corvallis, OR 97331, USA

[5]Department of Dermatology, Oregon Health & Science University (OHSU), Portland, OR 97239, USA

[6]Knight Cancer Institute, OHSU, Portland, OR 97239, USA

[7]Department of Surgery – Plastic & Reconstructive Surgery, University of Nebraska Medical Center, Omaha, NE 68198, USA

[8]Department of Surgery – General Surgery & Genetics, Cell Biology & Anatomy, University of Nebraska Medical Center, Omaha, NE 68198, USA

[9]Department of Surgery, VA Nebraska – Western Iowa Health Care System, Omaha, NE 68105, USA

[10]Department of Dermatology, University of California, San Diego, CA 92093, USA

*Author for correspondence: jingwei.xie@unmc.edu

**Author for correspondence: Adrian.Gombart@oregonstate.edu

Aim: The aim of this study was to develop a nanofiber-based dressing capable of local sustained delivery of 1α,25-dihydroxyvitamin D_3 (1,25$(OH)_2D_3$) and augmenting human *CAMP* induction. **Materials & methods:** Nanofibrous wound dressings containing 1,25$(OH)_2D_3$ were successfully prepared by electrospinning, which were examined *in vitro*, *in vivo* and *ex vivo*.**Results:** 1,25$(OH)_2D_3$ was successfully loaded into nanofibers with encapsulation efficiency larger than 90%. 1,25$(OH)_2D_3$ showed a sustained release from nanofibers over 4 weeks. Treatment of U937 and HaCaT cells with 1,25$(OH)_2D_3$-loaded poly(ϵ-caprolactone) nanofibers significantly induced hCAP18/LL37 expression in monocytes and keratinocytes, skin wounds of humanized transgenic mice and artificial wounds of human skin explants. **Conclusion:** 1,25$(OH)_2D_3$ containing nanofibrous dressings could enhance innate immunity by inducing antimicrobial peptide production.

First draft submitted: 11 January 2018; Accepted for publication: 16 March 2018; Published online: 4 July 2018

Keywords: 1α,25-dihydroxyvitamin D_3 • antimicrobial peptides LL-37 • electrospun nanofibers • endogenous production • innate immunity • sustained delivery

In the USA, over 290,000 surgical site infections (SSIs) occur within 30 days of an operation and kill more than 13,000 people each year [1–3]. These infections account for nearly US$10 billion annually in additional healthcare costs [2]. SSIs comprise 22% of all healthcare-associated infections (HAIs) and represent the most common HAIs among surgical patients [1–3]. These postsurgical infections increase the length of postoperative hospital stays by 7–10 days, rates of readmission to the hospital, expense and rates of death [4]. Treatment currently uses wound dressings that deliver antibiotics, but their use can select for survival of drug-resistant pathogens [5]. The majority of HAIs involve antibiotic-resistant ESKAPE pathogens (*Enterococcus faecium*, *Staphylococcus aureus*, *Klebsiella pneumoniae*, *Acinetobacter baumannii*, *Pseudomonas aeruginosa*, and *Enterobacter* species) [6]. The increasing frequency of multidrug-resistant bacterial species underscores the need for novel approaches with modes of action different from current antibiotics to bolster the antimicrobial regimens used to prevent SSIs.

Future Medicine

Electrospinning is a versatile, simple, cost-effective and reproducible technique for generating long fibers with nanoscale diameters [7]. Electrospun nanofiber wound dressings offer significant advantages over hydrogels or sponges for local drug delivery. It is difficult to encapsulate hydrophobic molecules inside hydrogels. In sponges, hydrophobic drug molecules usually crystalize after encapsulation, which slows down the dissolution rate and is unfavorable [8]. However, electrospun nanofibers offer ease of incorporation of drugs, particularly hydrophobic molecules, inside nanofibers, ease of control of release profiles, and exhibit an amorphous state for hydrophobic drug molecules, thus enhancing solubility of drugs [9,10]. Compared with traditional wound dressings, nanofiber-based wound dressings provide several functional and structural advantages including hemostasis, high filtration, semipermeability, conformability and scar-free healing [11,12]. Hydrogels are capable of soft-tissue-like compliance, but are difficult to suture and are often too weak to support physiologic loads [13]. Electrospun nanofibers offer numerous advantages, but their full potential has not been realized. There is a paucity of dressings that can simultaneously prevent or treat infections and promote wound healing [14]. Currently, their antimicrobial use is limited to surface modifications with chitosan and encapsulation of antibiotics or antimicrobial peptides, ZnO and silver nanoparticles/ions [12,15–17]. The use of these conventional single-target antimicrobial compounds could lead to the selection of drug resistance in a variety of microorganisms [18]. Also, increasing the local concentration of antimicrobial peptides through direct peptide application or over expression via gene therapy is frequently associated with toxicity to eukaryotic cells, inflammation and risk of undesired tissue damage in the area of the wound or surgical incision [19,20].

We and others showed that 1,25-dihydroxyvitamin D_3 ($1,25(OH)_2D_3$) induces expression of the *CAMP* gene, the encoded hCAP18 protein and secretion of the antimicrobial peptide LL-37 that is cleaved from the C-terminal end of hCAP18 in human monocytes, macrophages, dendritic cells, epithelial cells and skin keratinocytes [21–23]. This induction occurs only in humans and nonhuman primates because the vitamin D receptor response element (VDRE) is located on a retrotransposable *Alu*-element or short-interspersed nuclear element that is specific to primates [21,22]. Vitamin D does not induce mouse *Camp* gene expression because a VDRE does not exist in the mouse *Camp* promoter [21]. In humans, the regulation of *CAMP* expression could mediate, in part, the important barrier effects attributed to vitamin D [21,23,24]. Furthermore, LL-37 can significantly improve re-epithelialization and granulation of tissue in excisional wounds of mice [24,25]. Enhancement of innate immunity by inducing antimicrobial peptide production, like LL-37, could mitigate the selection for multidrug resistance and improve wound healing, and the immune-modulating properties of vitamin D could mitigate the development of excessive inflammation [26]. Furthermore, we recently demonstrated the successful encapsulation of immune-modulating compounds such as 25-hydroxyvitamin D_3 ($25(OH)D_3$) (the primary circulating form of vitamin D) in electrospun nanofibers that elicited a durable release of encapsulated compounds over 28 days and induction of antimicrobial peptide expression *in vitro* [27,28]. Herein, we for the first time demonstrated the local sustained delivery of $1,25(OH)_2D_3$ (an active and more potent form of vitamin D) by biocompatible and biodegradable nanofibrous dressings to induce endogenous antimicrobial peptide hCAP18/LL-37 expression in keratinocytes, monocytes/macrophages, humanized transgenic mice skin wounds and *ex vivo* human skin wounds.

Materials & methods

Fabrication & characterization of $1,25(OH)_2D_3$-loaded nanofibers

$1,25(OH)_2D_3$ (Santa Cruz Biotechnology Inc., TX, USA) was encapsulated in poly(ϵ-caprolactone) (PCL; molecular weight (Mw) = 70–90 kDa, Sigma-Aldrich, MO, USA) nanofibers using electrospinning as described in our previous studies [10,29]. Briefly, PCL was dissolved in a solvent mixture consisting of dichloromethane (Thermo Fisher Scientific, MA, USA) and dimethylformamide (Thermo Fisher Scientific) with a ratio of 4:1 (v/v) at a concentration of 9% (w/v). To enhance the hydrophilicity of fibers, 1% (w/v) pluronic F-127 (Sigma-Aldrich) was added to the solution. The stock solution of $1,25(OH)_2D_3$ was prepared by dissolving 1 mg $1,25(OH)_2D_3$ in 1 ml DMSO (Thermo Fisher Scientific) and added to the polymer (PCL) solution with an initial drug loading of 250 ng/g. The polymer solution was pumped at a flow rate of 0.6 ml per hour using a syringe pump, while an electrical potential of 15 kV was applied between the spinneret (a 22-gage needle) and a grounded collector located 15 cm from the spinneret. A rotating drum collected membranes composed of random fibers with a rotating speed less than 100 rpm. The morphology and diameter of the nanofiber samples were characterized by a scanning electron microscope (SEM; FEI, Quanta 200, OR, USA) following our previous studies [10,29]. The porosity and mechanical properties of nanofiber mats were reported in our previous studies [30,31].

In vitro release of $1,25(OH)_2D_3$ from the fibers was evaluated by immersing 10-mg fiber samples in 10-ml phosphate-buffered saline (PBS) at 37°C. The supernatants were collected at each time point and replaced with fresh PBS. Drug loading and encapsulation efficiency were determined following our previous procedures [27]. $1,25(OH)_2D_3$-loaded fiber samples were first dissolved in glacial acetic acid at the concentration of 10 mg/ml, and then the solutions were diluted for 100-times with glacial acetic acid, and further diluted for 100-times with PBS. The $1,25(OH)_2D_3$ concentrations of collected samples were determined using a $1,25(OH)_2D_3$ ELISA kit according to the manufacturer's instructions (Cayman Chemical, CA, USA).

Nanofibers were sterilized by AN 74i ethylene oxide (EO) for 12 h, formaldehyde vapor at 1.0×10^{-1} Pa for 12 h or γ-irradiation at 15 kGy. To test the activity of the released $1,25(OH)_2D_3$, a 10-mg sample of $1,25(OH)_2D_3$-loaded PCL nanofibers prior to sterilization and the same amount of each sterilized sample was immersed in 10-ml PBS at 37°C for 1 h. The activity of released $1,25(OH)_2D_3$ was determined using a reporter assay for the human vitamin D receptor (VDR) as instructed by the manufacturer (Indigo Biosciences, PA, USA). The relative activity of released $1,25(OH)_2D_3$ from each fiber samples was expressed as percentages relative to the activity of released $1,25(OH)_2D_3$ from the nanofiber sample prior to sterilization.

Cell culture & treatments

The human keratinocyte cell line HaCaT and monocyte cell line U937 were cultured in Dulbecco's Modified Eagle's Medium (DMEM) with 10% fetal bovine serum (FBS) and RPMI-1640 media with 10% FBS, respectively. The cultures were maintained at 37°C with 5% CO_2. Upon reaching 80% confluent growth, HaCaT cells were dissociated with 0.05% trypsin-EDTA and resuspended by gentle pipetting in fresh complete media. Cells were seeded in 6-cm dishes at 5.0×10^5, 2.0×10^5 and 1.0×10^5 cells for 1-, 3- and 5-day treatments, respectively. After 1 day of growth, the media was then replaced by DMEM (Control [Ctr]), DMEM containing 0.52% DMSO, DMEM (Thermo Fisher Scientific) containing 2.0×10^{-7} M $1,25(OH)_2D_3$, DMEM containing 1 mg/ml pristine PCL fibers and DMEM containing 1 mg/ml $1,25(OH)_2D_3$-loaded PCL fibers and incubated for 1, 3 and 5 days. U937 cells were pelleted by 300× *g* centrifugation for 5 min and then resuspended in fresh complete media. Cells were seeded in 6-cm culture dishes. Cells were incubated with Roswell Park Memorial Institute (RPMI)-1640 (Ctr), RPMI-1640 containing 0.52% DMSO, RPMI-1640 containing 2.0×10^{-7} M $1,25(OH)_2D_3$, RPMI-1640 containing 1 mg/ml pristine PCL fibers and RPMI-1640 containing 1 mg/ml $1,25(OH)_2D_3$-loaded PCL fibers for 1, 3 and 5 days. All the nanofiber samples were sterilized by γ-radiation at a dose of 15 kGy prior to use for both *in vitro* and *in vivo* tests.

In vitro antimicrobial peptide induction

After treatments with different formulations, U937 and HaCaT cells were rinsed with PBS twice and fixed with 4% paraformaldehyde (Thermo Fisher Scientific) for 30 min at 37°C followed by incubation with 2,4,6-trinitrobenzenesulfonic acid solution (TNBS) (0.05% Triton-X100, 2% FBS in pH 7.2 PBS; Thermo Fisher Scientific) for 30 min at room temperature prior to immunostaining. Fixed and permeabilized cells were incubated overnight at 4°C with goat anti-LL37 polyclonal antibody diluted 1:200 (Santa Cruz Biotechnology Inc.). After removal of the primary antibody, cells were washed three-times with TNBS and incubated for 2 h with mouse anti-goat IgG-Dylight 488 antibody (Abcam, MA, USA) diluted 1:100. The secondary antibody was removed and cells washed three-times with TNBS. Nuclei were counterstained with 10 μM 4′,6-diamidino-2-phenylindole (DAPI). Images were taken with a digital camera (Carl Zeiss). The exposure time for taking images for U937 and HaCaT cells was fixed at 40 ms and 400 ms, respectively. To determine the relative expression levels for the treated cells, fluorescence-activated cell sorting was performed on a FACSCalibur flow cytometer (Becton Dickinson, NJ, USA). U937 and HaCaT cells were fixed and stained following the procedures described above. DAPI counterstaining was omitted. We collected a total 10,000 events for each sample, results were analyzed using BD Cell Quest (BD Biosciences, CA, USA) and cell immunofluorescence was determined using the standard FlowJo software (FlowJo LLC, OR, USA).

To quantify the induction of hCAP18/LL-37, HaCaT and U937 cells were seeded in 6-cm culture dishes at 5.0×10^5, 2.0×10^5 and 1.0×10^5 cells, and incubated for 1, 3 and 5 days and treated with different formulations as described above. Subconfluent HaCaT cells and U937 cell suspensions were washed with PBS twice, pelleted and resuspended in 300 μl of the M-PER mammalian protein extraction reagent (Thermo Fisher Scientific) containing 0.1% protease inhibitor cocktail (Sigma-Aldrich). The total protein concentration was quantified using

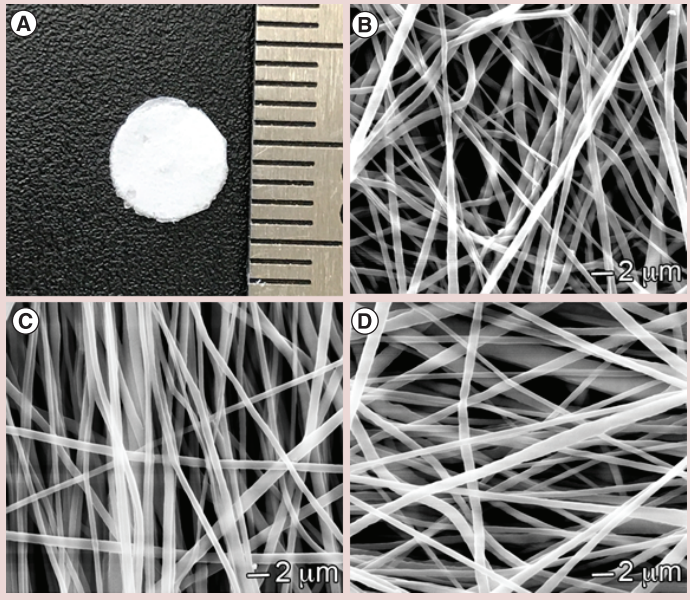

Figure 1. Morphology characterization. (A) Photograph shows a 1,25$(OH)_2D_3$-loaded PCL fiber membrane with a diameter of 5 mm. **(B & C)** SEM images of **(B)** PCL fibers, **(C)** 1,25$(OH)_2D_3$-loaded PCL fibers and **(D)** 1,25$(OH)_2D_3$-loaded PCL/pluronic F127 fibers.
PCL: Poly(ϵ-caprolactone); SEM: Scanning electron microscope.

a MicroBCA assay kit (Thermo Fisher Scientific). The level of hCAP18/LL-37 expression in each cell lysate was determined using an ELISA assay kit as instructed by the manufacturer (Hycult Biotech, PA, USA).

In vivo full-thickness wounding in mice

All the mice used were bred and maintained in the same temperature (23 ± 1°C), humidity (50–60%) and lighting (6:00 am–6:00 pm) controlled rooms under specific pathogen-free conditions. Full-thickness skin wounds were generated as described previously [32,33]. Briefly, 6–8-week-old littermate mice were anesthetized and 4-mm diameter punch biopsies were generated on each flank. The skin from one wound was fixed in RNA later for RNA isolation and the other was fixed in paraformaldehyde for tissue section and histopathology. Nanofibrous dressings (5-mm diameter discs) were implanted inside the wound with edges tucked under the wound edge (Figure 1A). Wounds were then covered with Nexcare™ Tegaderm™ Waterproof Transparent Dressing to secure the disc inside the wounds (3M, MN, USA). On day 3, mice were euthanized and the wound area was resected including 2 mm of the wound border and excised for histology and immunohistochemical/immunofluorescence analyses. One wound was fixed in RNAlater (Thermo Fisher Scientific) for RNA isolation and stored at -80°C. A distal skin sample from the neck area of each animal was collected for RNA isolation. The mice were either *Camp*-null (*Camp* $^{KO/KO}$) or dizygous for the human *CAMP* gene (*CAMP* $^{Tg+/Tg+}$) on a *Camp*$^{KO/KO}$ background [34]. The latter mice are designated as *CAMP* $^{Tg+/Tg+}$:*Camp* $^{KO/KO}$.

RNA isolation & qRT-PCR analysis of gene expression

Total RNA was isolated using a Direct™-zol RNA kit according to the manufacturer's protocol (Zymo Research Corp., CA, USA). Tissues were homogenized using nuclease-free 1.6-mm stainless steel beads in a Precellys24 homogenizer (Bertin Corp., MD, USA). RNA (0.125 µg) was converted to cDNA using iScript reverse transcriptase and random hexamer primers as instructed by the manufacturer (Bio-Rad Laboratories, CA, USA). PCR reactions were performed with SsoAdvanced Universal Probes Supermix as instructed by the manufacturer (Bio-Rad Laboratories). PCR was performed on a Bio-Rad CFX-96 QPCR system (Bio-Rad Laboratories). The primers and probe for the human *CAMP* gene used for quantitative real time (qRT)-PCR were described previously [35]. All the threshold cycle (C_t) numbers were normalized to the reference gene, *Ywhaz* that we determined to be relatively

stable in both normal and wounded skin (data not shown). Primers and probe for *Ywhaz* were purchased (Integrated DNA Technologies, IA, USA).

Immunofluorescence analysis

Paraffin-embedded sections were used for immunofluorescence antibody staining as described previously [32,33]. Briefly, sections were incubated with 10% serum for 1 h to block nonspecific binding and incubated with rabbit anti-hCAP18 antibody overnight (1:500) at 4°C. Slides were then washed three-times and incubated with fluorescently labeled Cy3 (1:500; Jackson ImmunoResearch) secondary antibody for 2 h at 37°C. Nuclei were counterstained with DAPI. Images were captured at 20× magnification using a Leica Digital Modulation Recognition Algorithm (DMRA) fluorescence microscope and Hamamatsu C4742–95 digital camera.

Ex vivo antimicrobial peptide induction in human skin tissue

The human skin tissues were collected from patients who underwent plastic surgery. All the samples were incubated with DMEM within 2 h after surgery. The full skin tissue was cut into 2 cm × 2 cm sections. PCL was formed in a sheet with a size of 2 cm × 2 cm × 0.2 cm using a customized mold. The tissue was fixed on the PCL sheet by three or four staple clips at the corners of each tissue and then placed in a 6-cm diameter culture dish. Approximately 7 ml DMEM medium with 10% FBS was added to each dish to maintain the dermal layer in contact with the medium and the epidermal layer exposed to the air. After incubation for 1 day, a 1-mm deep wound was generated in the center of each skin fragment using an 8-mm diameter punch. Nanofiber discs were cut using an 8-mm diameter punch and inserted into each wound. Both the wound tissue and 2-mm border from around the wound were harvested using a 10-mm punch at various time points and homogenized in 0.5-ml tissue lysis buffer at 4°C. The tissue homogenate was centrifuged at 14,000 rpm for 20 min at 4°C. After centrifugation, the liquid separated into three layers including lipid, supernatant and precipitate from the top to the bottom. The amount of hCAP18/LL-37 in 100 µl of supernatant was determined by ELISA as described above.

Statistical analysis

The data were presented as the mean ± standard deviation, and statistical analysis was performed using SPSS 13.0 and GraphPad 7.0 software. T-test and one-way analysis of variance with Tukey's multiple comparison post-test were used to determine significance. The values of p less than 0.05 were considered statistically significant, and the values of p less than 0.01 were considered statistically very significant.

Results

Fabrication & characterization of $1,25(OH)_2D_3$-loaded nanofibers

The rationale for encapsulating $1,25(OH)_2D_3$ in nanofibers is to ensure sustained delivery of $1,25(OH)_2D_3$ at the wound site. In U937 monocyte cells, the absence of sustained delivery of $1,25(OH)_2D_3$ results in a rapid drop in the expression of induced *CAMP* mRNA levels (Supplementary Figure 1). These findings suggest that repeated application of $1,25(OH)_2D_3$ at a wound site could be necessary to ensure continued expression of *CAMP* in the wound. PCL was selected as carrier material because it is a biocompatible and biodegradable polymer that has been approved by the US FDA for certain clinical applications [36]. In this study, PCL nanofibers were served as dressing material for releasing $1,25(OH)_2D_3$ molecules in a sustained manner instead of serving as scaffold for cell infiltration and tissue regeneration. Therefore, the degradation of PCL nanofibers was not considered. Nanofiber formulations were fabricated by electrospinning. Figure 1A shows a photograph of 5-mm nanofiber disc for implantation to the wounds. SEM images of PCL, $1,25(OH)_2D_3$-loaded PCL and $1,25(OH)_2D_3$-loaded PCL/pluronic F127 nanofibers demonstrated that they possess a cylindrical shape with a smooth surface and diameters ranging from about 300 nm to 1 µm (Figure 1B–D). The drug loadings for $1,25(OH)_2D_3$-loaded PCL and PCL/pluronic F127 nanofibers were 243 ± 8 and 233 ± 14 ng/mg, respectively. And the corresponding encapsulation efficiencies were 97.2 ± 3.2% and 93.2 ± 5.6%. The addition of pluronic F127 resulting in a slight decrease in encapsulation efficiency could be due to the possible occurrence of phase separation of electrospinning solutions as pluronic F127 is amphiphilic.

To determine the release kinetics of $1,25(OH)_2D_3$ from PCL fibers and PCL/pluronic F127 fibers, we incubated the nanofibers in PBS and determined the amount of $1,25(OH)_2D_3$ released into solution for 28 days. The release profiles exhibited an initial burst followed by a sustained release over 28 days (Figure 2). The additive of pluronic F127 can accelerate the release rate, which could be due to the water solubility of pluronic F127 that results in more

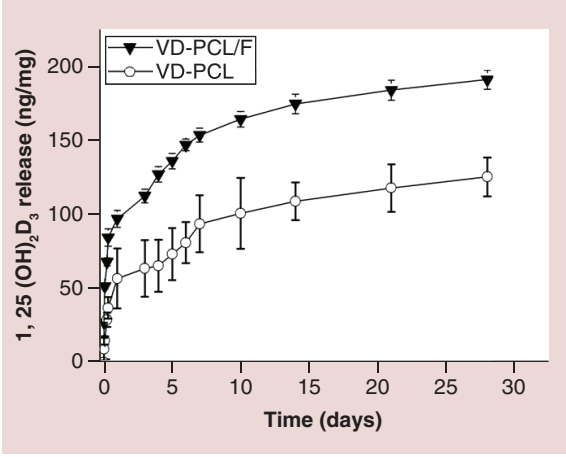

Figure 2. *In vitro* release kinetics of $1,25(OH)_2D_3$. Release profiles of VD from VD-PCL membranes and VD-PCL/pluronic F127 nanofiber (VD-PCL/F) membranes. Each data point represents the arithmetic mean ± standard deviation values from three samples. F: Plutonic F127; PCL: Poly(ϵ-caprolactone); VD-PCL: $1,25(OH)_2D_3$-loaded PCL nanofiber.

pores on the nanofibers after immersion in aqueous solutions. It is observed that 125 and 175 ng $1,25(OH)_2D_3$ was released from 1 mg of $1,25(OH)_2D_3$-loaded PCL and PCL/pluronic F127 nanofiber mats, respectively, after incubation for 28 days.

To determine the most effective sterilization method, the activity of $1,25(OH)_2D_3$ released from fibers was tested. We sterilized the fiber formulations using EO, formaldehyde vapor or γ-irradiation. The activity of $1,25(OH)_2D_3$ decreased dramatically to 1.0% after EO sterilization (Supplementary Figure 2) and about 20% activity after formaldehyde sterilization compared with the unsterilized nanofibers. In contrast, the $1,25(OH)_2D_3$ released from the γ-irradiation-sterilized fiber formulation maintained about 60% activity relative to the unsterilized formulation. This was significantly higher than the other two sterilization methods and γ-irradiation was used to sterilize the fibers for subsequent *in vitro* and *in vivo* work.

Induction of antimicrobial peptide expression *in vitro*

We subsequently examined the capability of various formulations to induce the expression of hCAP18/LL-37 in U937 monocyte and HaCaT cells (Figures 3 & 4). Both monocytes and keratinocytes play an important role in the response of wounding and expressing CAMP. We used a polyclonal anti-hCAP18/LL-37 antibody and Dylight 488-conjugated secondary antibody to perform immunofluorescence staining and qualitatively examine the effects of different formulations on protein expression. The primary antibody detects both the full length and cleaved C terminus (LL-37) of hCAP18. As expected, DMSO and pristine PCL fibers were incapable of inducing hCAP18/LL-37 expression in U937 and HaCaT cells (Figures 3 & 4). In U937 cells, we observed marginally positive staining of hCAP18 after 1-day treatment with 2.0×10^{-7} M $1,25(OH)_2D_3$ and 1 mg/ml $1,25(OH)_2D_3$-loaded PCL fibers (Figure 3). Based on the release profile data, the fibers would release about 2.0×10^{-7} M $1,25(OH)_2D_3$ by day 3. With increased incubation time, the fluorescent intensity of cells increased when treated with 2.0×10^{-7} M $1,25(OH)_2D_3$ and 1 mg/ml $1,25(OH)_2D_3$-loaded PCL fibers (Figure 3). Treatment with 1 mg/ml $1,25(OH)_2D_3$-loaded PCL fibers appeared to induce more hCAP18/LL-37 than the treatment with free 2.0×10^{-7} M $1,25(OH)_2D_3$ at days 3 and 5 (Figure 3). HaCaT cells showed a similar result (Figure 4). We further confirmed this result using flow cytometry (Figures 3 & 4). On day 1, the fluorescent intensity of U937 cells for the control group and treatment groups were similar. With increasing incubation time, the peak fluorescence of U937 cells shifted to the right after administration of 2.0×10^{-7} M $1,25(OH)_2D_3$ and 1 mg/ml $1,25(OH)_2D_3$-loaded PCL fibers. After treatment for 3 and 5 days, the peak fluorescence in U937 cells treated 1 mg/ml $1,25(OH)_2D_3$-loaded PCL fibers was the highest compared with the control, PCL and free $1,25(OH)_2D_3$ treatment groups (Figure 3). A similar trend was observed in HaCaT cells after incubation with $1,25(OH)_2D_3$-loaded PCL fibers for 5 days relative to the control and other treatment groups (Figure 4). The additive of pluronic F-127 slightly enhanced the induction of human CAMP compared with nanofibers without it (Supplementary Figure 1, lower panel). This was expected as the pluronic F-127 additive would enhance release of $1,25(OH)_2D_3$.

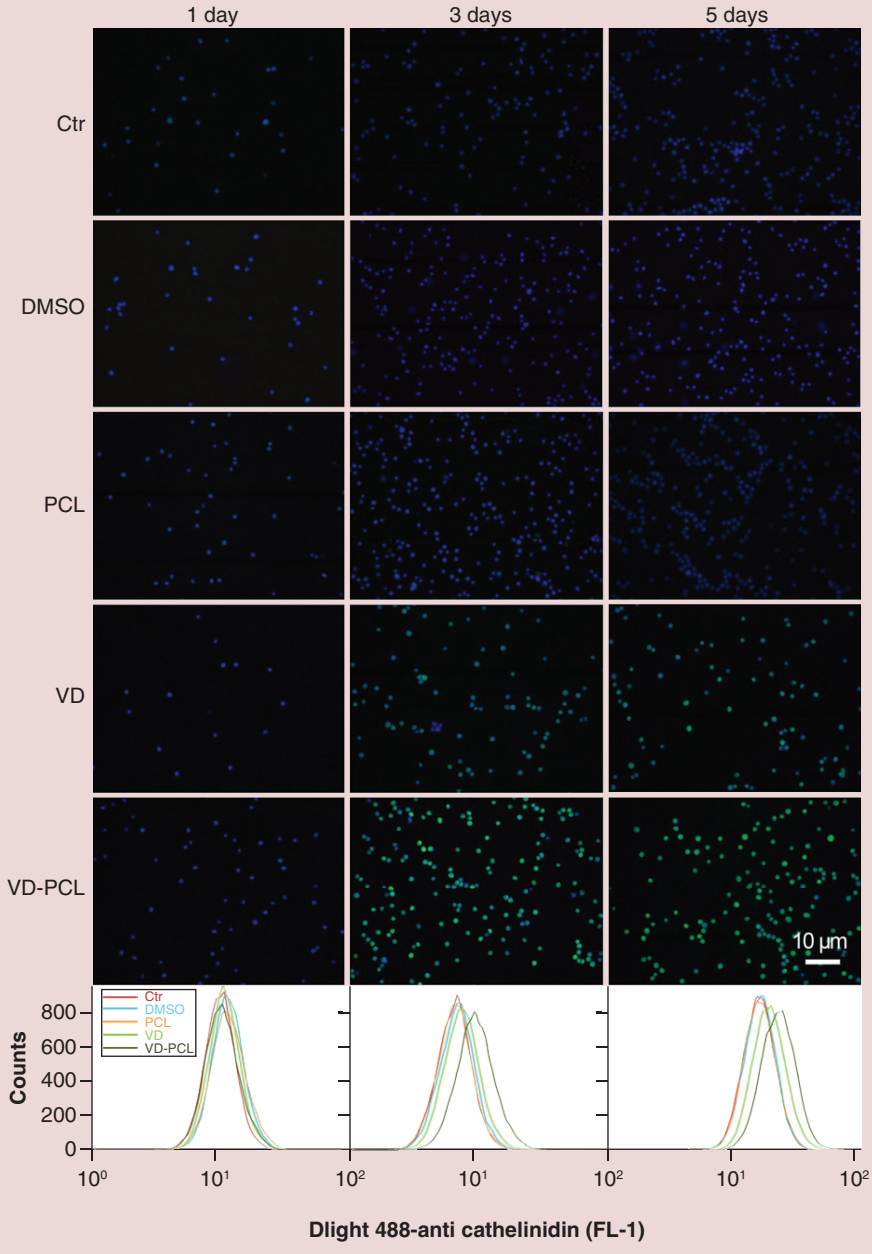

Figure 3. $1,25(OH)_2D_3$-loaded poly(ϵ-caprolactone) nanofibers induce hCAP18/LL37 protein expression.
Immunofluorescent staining with anti-hCAP18 antibody shows the expression of cathelicidin in U937 cells that were incubated in the absence (Ctr: without any treatment) and presence of pristine 1 mg/ml PCL fibers, 0.52% DMSO, 2.0×10^{-7} M VD or VD-PCL fibers for 1, 3 and 5 days. Expression levels were determined by flow cytometry (lower panels).
Ctr: Control; DMSO: Dimethyl sulfoxide; PCL: Poly(ϵ-caprolactone); VD: $1,25(OH)_2D_3$.

Quantification of induced antimicrobial peptide *in vitro*

We quantified the induction of antimicrobial peptide from HaCaT and U937 cells after coincubation with different formulations using an hCAP18/LL-37 ELISA kit (Figures 4 & 5). The induction of hCAP18/LL-37 in U937 cells was significantly higher when incubated with 1 mg/ml $1,25(OH)_2D_3$-loaded PCL fibers for 3 and 5 days than the control and free drug (Figure 5). Similarly, administration of 1 mg/ml $1,25(OH)_2D_3$-loaded PCL fibers induced the highest amount of hCAP18/LL-37 in HaCaT cells among the treatment groups after incubation for 5 days

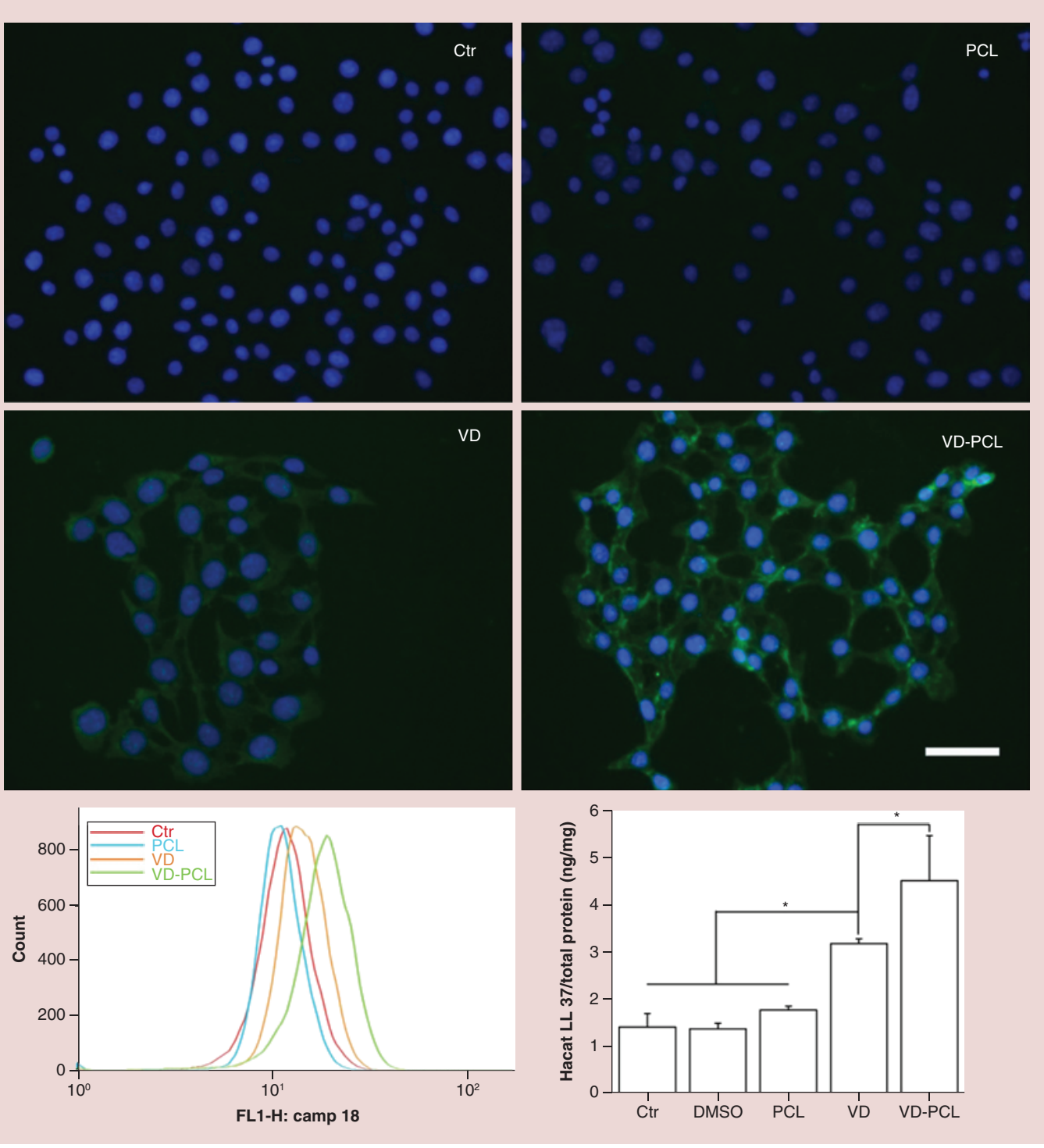

Figure 4. hCAP18/LL37 expression is induced in HaCaT cells after treatment with VD-PCL fibers. Fluorescence microscopy images show hCAP18/LL37 expression in HaCaT cells that were incubated in the presence of 0.52% DMSO (Ctr: treatment with 0.52% DMSO), pristine 1 mg/ml PCL fibers, 2.0×10^{-7} M VD and 1 mg/ml VD-PCL fibers for 5 days.
Ctr: Control; DMSO: Dimethyl sulfoxide; PCL: Poly(ϵ-caprolactone); VD: $1,25(OH)_2D_3$.

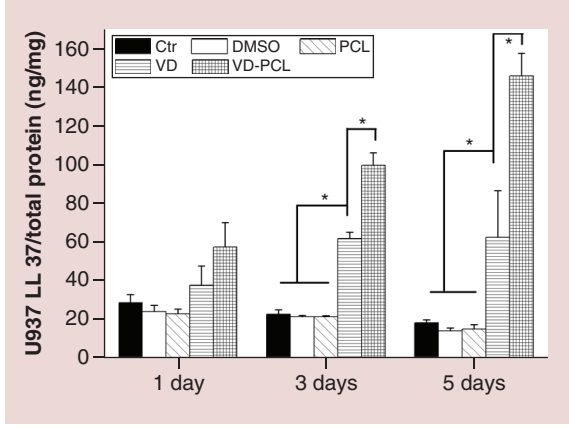

Figure 5. Quantification of hCAP18/LL-37 expressed in U937 cells after treatment with different formulations. Cells were incubated in the absence (Ctr: without any treatment) and presence of 1 mg/ml pristine PCL fibers, 0.52% DMSO, 2.0×10^{-7} M VD or 1 mg/ml VD-PCL fibers for 1, 3 and 5 days. The levels of hCAP18/LL-37 were measured by ELISA. Each data point represents the arithmetic mean ± standard deviation values from three samples. Statistical significance was evaluated by one-way analysis of variance (*$p < 0.05$).
Ctr: Control; DMSO: Dimethyl sulfoxide; PCL: Poly(ϵ-caprolactone); VD: $1,25(OH)_2D_3$.

(Figure 4). In addition, U937 cells produced a tenfold higher amount of hCAP18/LL-37 than HaCaT cells under the same conditions.

Induction of *CAMP* gene expression in transgenic *Camp* mice

We hypothesized that nanofibrous dressings would provide local release of $1,25(OH)_2D_3$, and induce expression of hCAP18/LL-37 in full-thickness skin wounds *in vivo*. To test this, we performed a full-thickness wound assay in *CAMP* $^{Tg+/Tg+}$:*Camp*$^{KO/KO}$ mice. Due to the limited fluid in the wound site (unlike the *in vitro* environment), we chose pluronic F127 as an additive to fibers for enhancing hydrophilicity and the release rate. After wounding, either PCL or $1,25(OH)_2D_3$-loaded PCL/pluronic F127 nanofibers were inserted in the wound bed. At day 3 postwounding, we collected the wound skin, skin distal to the wound and the kidneys for mRNA and/or protein expression analyses (Figure 6A). Quantitative RT-PCR for *Cyp24a1* expression in the kidney demonstrated that some of the $1,25(OH)_2D_3$ released by the nanofibers entered the circulation and induced this gene as expected (Figure 6B). *CAMP* gene expression was significantly induced in the wounds by $1,25(OH)_2D_3$-loaded PCL/pluronic F127 nanofibers when compared with the skin taken from the wound on day 0 or skin from a distal site collected on day 3 (Figure 6C). Also, *CAMP* was induced significantly in wounds on day 3 treated with $1,25(OH)_2D_3$-loaded PCL/pluronic F127 nanofibers when compared with those treated with PCL nanofibers (Figure 6D). Taken together, the data indicate that $1,25(OH)_2D_3$ is released from the loaded fibers and induction of *CAMP* is limited to the area of the wound and not skin at distal sites.

Consistent with lower mRNA expression, immunofluorescence staining confirmed low expression of hCAP18/LL-37 in cells of the dermis of the unwounded skin (Figure 6, left panel). This staining was not observed in skin from the *Camp*$^{KO/KO}$ mice or in skin from *CAMP* $^{Tg+/Tg+}$:*Camp*$^{KO/KO}$ mice upon omission of the hCAP18 antibody (Supplementary Figure 4). At day 3, hCAP18 expression increased in the PCL-treated wound (Figure 7, middle panel) consistent with induction of hCAP18 upon wounding. In the presence of $1,25(OH)_2D_3$-loaded PCL nanofibers, we observed a dramatic increase in hCAP18/LL-37 expression in the wound bed (Figure 7, right panel vs middle panel and corresponding lower insets). By quantifying the fluorescent intensity, we observed 126% increase in hCAP18 expression postwounding and a further increase to 141% was observed with $1,25(OH)_2D_3$ containing nanofibers. Staining for a macrophage/monocyte-specific cell surface marker, F4/80, indicated that this was due in part to a significant increase of infiltrating immune cells that were also expressing higher levels of hCAP18/LL-37 induced by the $1,25(OH)_2D_3$ (Supplementary Figure 5). We counted the cells expressing the hCAP18 in the dermis and represented as hCAP18-positive cells per field. We plotted them as bar graph (Supplementary Figure 6). A significantly higher number of hCAP18-positive cells per field were observed for the group treated by $1,25(OH)_2D_3$-loaded PCL/pluronic F127 nanofibers than the one treated by pristine fibers. Taken together, the results indicate that $1,25(OH)_2D_3$-loaded PCL/pluronic F127 nanofibers increase the infiltration of immune cells and induce expression of hCAP18 in those cells during cutaneous wound healing.

Ex vivo antimicrobial peptide production & histological analysis

We examined the ability of nanofiber formulations to induce hCAP18/LL-37 expression in *ex vivo* human skin tissue. A $1,25(OH)_2D_3$-loaded PCL fiber membrane was placed in a 1-mm deep wound in human skin (Figure 8A

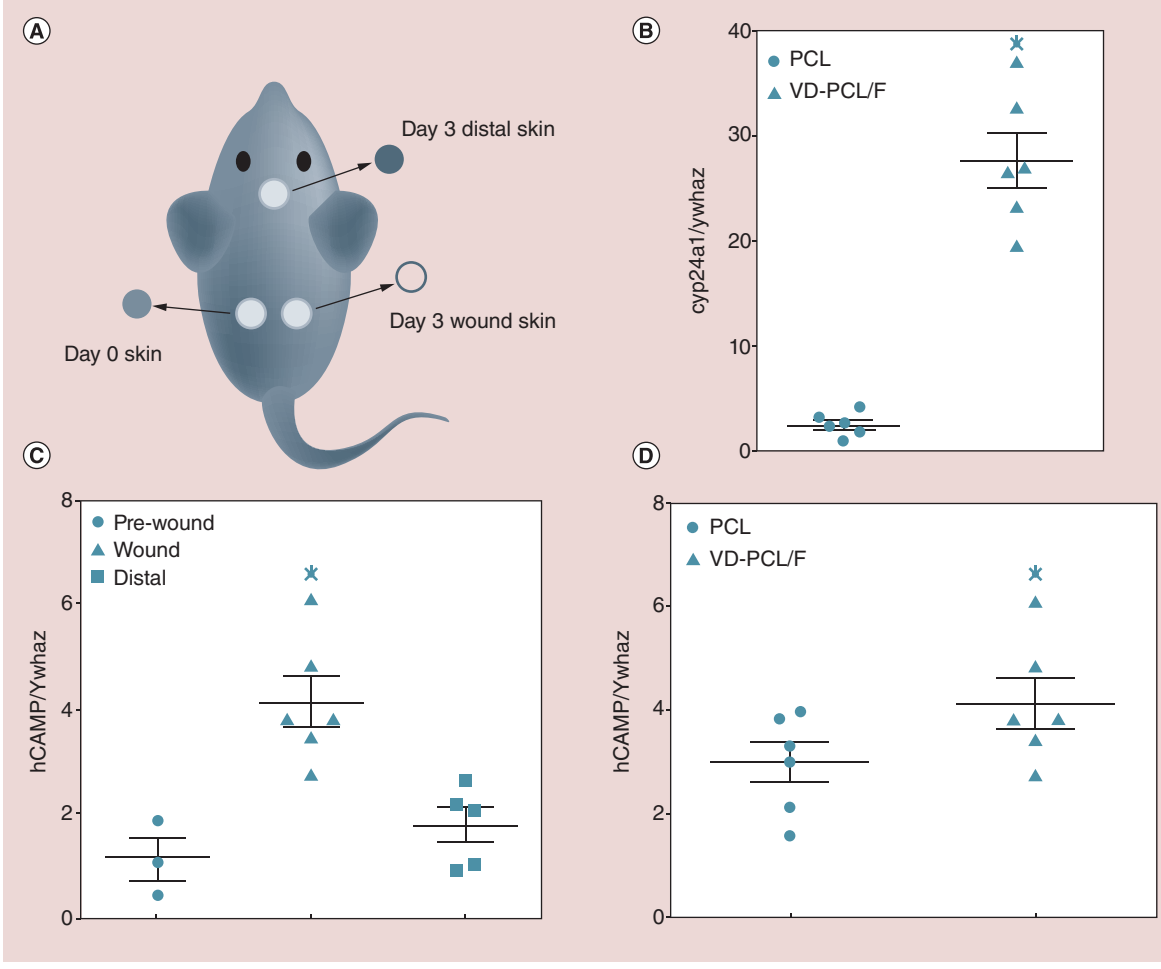

Figure 6. 1,25(OH)$_2$D$_3$-loaded poly(ϵ-caprolactone)/pluronic F127 nanofiber (VD-PCL/F) dressings induce *CAMP* gene expression in full-thickness excisional wounds in human *CAMP* $^{Tg+/Tg+}$; murine *Camp*$^{KO/KO}$ mice 3 days postwounding. (A) Schematic showing location of nanofiber dressings in the wounds on each flank, the day 0 skin taken from the wound and the skin distal from the wound collected on day 3. **(B)** *Cyp24a1* mRNA expression in the kidneys of mice treated with PCL or VD-PCL/F dressings collected on day 3. **(C)** *CAMP* mRNA expression in the day 0 skin, wound and skin distal to the wounds in mice treated with VD-PCL/F dressings. **(D)** *CAMP* mRNA expression in wounds containing PCL nanofibers (PCL) versus expression in wounds containing VD-PCL/F. Data are means ± SEM of two independent experiments (n = 6) and are normalized to mouse *Ywhaz* and expressed as a ratio. Panels **(B)** and **(D)**, $p < 0.05$ by paired *t*-test. Panel **(C)**, $p < 0.01$ by one-way analysis of variance and Tukey's multiple comparisons test. Statistical significance indicated by *$p < 0.05$.
F: Pluronic F127; PCL: Poly(ϵ-caprolactone); SEM: Scanning electron microscopy; VD: 1,25(OH)$_2$D$_3$.

& B) and cultured for 1, 3 and 5 days (Figure 8C). The 1,25(OH)$_2$D$_3$-loaded PCL fibers induced hCAP18/LL-37 in the wound to a significantly higher level at days 1, 3, and 5 as compared with the control groups (Figure 8D). The level of hCAP18/LL-37 increased over time with the highest levels observed at day 5.

Discussion

During wound healing, keratinocytes, fibroblasts, endothelial and immune cells communicate with each other to regulate the expression of numerous cytokines, chemokines, antimicrobial proteins/peptides and growth factors to speed the healing process and prevent infection [37,38]. The VDR is a transcription factor that forms a heterodimer with retinoid X receptor and in the presence of 1,25(OH)$_2$D$_3$ it binds to VDREs in the promoters of target genes and modulates their expression [39,40]. Primary human keratinocytes treated with 1,25(OH)$_2$D$_3$ differentially express 50 responsive genes with the majority being novel targets in primary keratinocytes [41]. One of five enriched clusters includes genes involved in wounding/inflammatory responses [41]. We and others discovered

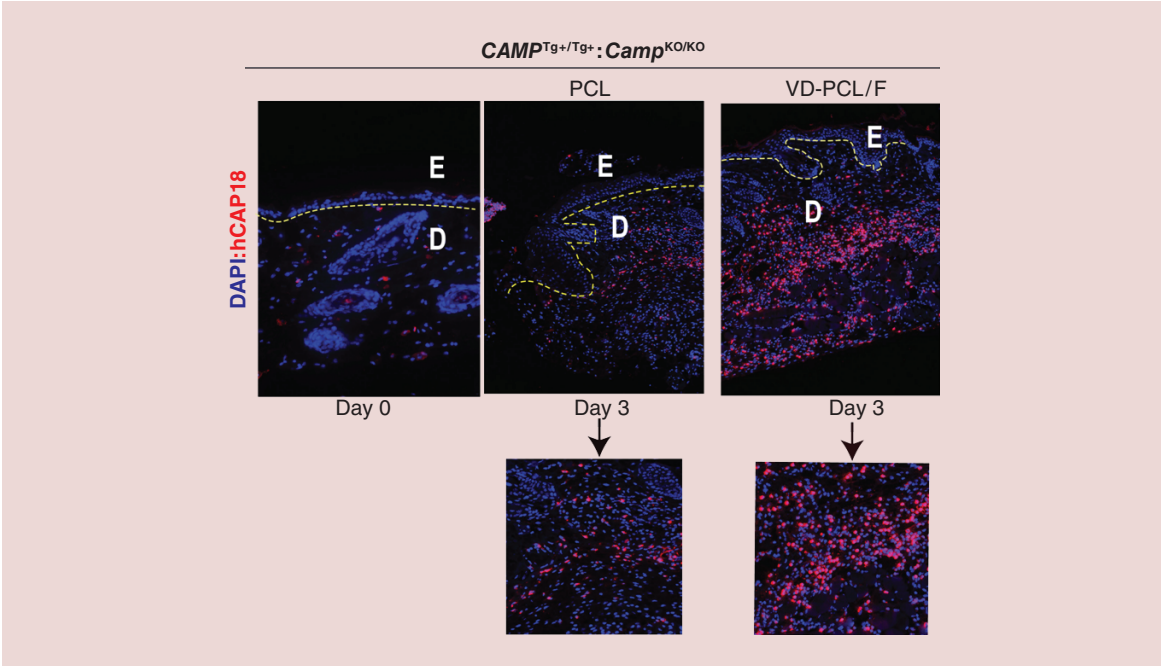

Figure 7. Induction of hCAP18/LL-37 protein in the dermis postwounding of the human *CAMP* transgenic mouse.
Immunofluorescence staining of hCAP18/LL-37 protein (in red) on day 3 samples in the presence of PCL fibers with or without $1,25(OH)_2D_3$. Nuclei were counterstained with DAPI (in blue). The yellow-dotted lines indicate the separation of the epidermis (E) from the dermis (D). Insets indicate higher magnification (40×) images of hCAP18/LL-37 protein expression in the absence (left) or presence (right) of $1,25(OH)_2D_3$. Original magnifications: 10×.
DAPI: 4′,6-diamidino-2-phenylindole; PCL: Poly(ϵ-caprolactone).

that $1,25(OH)_2D_3$ induces CAMP expression in human monocytes, macrophages, dendritic cells, keratinocytes and skin [21,23,42,43]. Normal, unwounded skin expresses undetectable levels of CAMP in human and mice, but abundant levels rapidly appear in the dermis at the edge of the wound and at later times postwounding in the granulation tissue and crust [42]. Basal keratinocytes express very low levels of hCAP18/LL-37 that increase after injury or during inflammation [44–46]. Our results are consistent with these prior findings as we observed very low levels of hCAP18/LL-37 in the unwounded skin of transgenic mice and significant upregulation in the dermis following wounding (Figures 6 & 7; Supplementary Figures 4 & 5).

After skin injury, the activated VDR induces expression of the inactive pro-protein hCAP18, TLR2 and CD14 [47]. Increased TLR2 and CD14 expression enhances keratinocyte responses to invading microbes that further increases *CAMP* gene expression. Upon cleavage by serine proteases, cells release the bactericidal cationic peptide LL-37 that effectively kills methicillin-resistant *Staphylococcus aureus* and may fight other drug-resistant bacterial infections [48,49]. In humans, induction of *CAMP* mRNA and hCAP18/LL-37 protein was observed in the epidermis adjacent to the wound and by the second day, it was observed in the migratory tongue during the re-epithelialization stage [50]. In the epithelium of chronic wound ulcers, hCAP18/LL-37 is absent in the ulcer edge epithelium suggesting that *CAMP* expression is important for proper wound healing [44]. *Camp*-deficient mice are susceptible to necrotic skin infections caused by Group A *Streptococcus* and decreased expression of cathelicidin also allows increase entry of *S. aureus* through the epidermal barrier [50,51].

Physiological upregulation of hCAP18/LL-37 expression in normal skin and acute skin wounds is accelerated by topical application of calcipotriol, a $1,25(OH)_2D_3$ analog [24,43]. In this study, we demonstrate that release of $1,25(OH)_2D_3$ from nanofibrous dressings induces localized *CAMP* mRNA and hCAP18/LL-37 expression in the wound (Figures 5 & 6). Much of the increased expression appeared to be due to increased production of hCAP18/LL-37 in macrophages and increased recruitment of macrophages expressing high levels of hCAP18/LL-37. The release of $1,25(OH)_2D_3$ from these PCL nanofibers allows durable long-term release that avoids the need for repeated application of $1,25(OH)_2D_3$. We showed that without the constant presence of $1,25(OH)_2D_3$ CAMP induction rapidly drops to uninduced levels (Supplementary Figure 1). This study outlines a strategy to develop

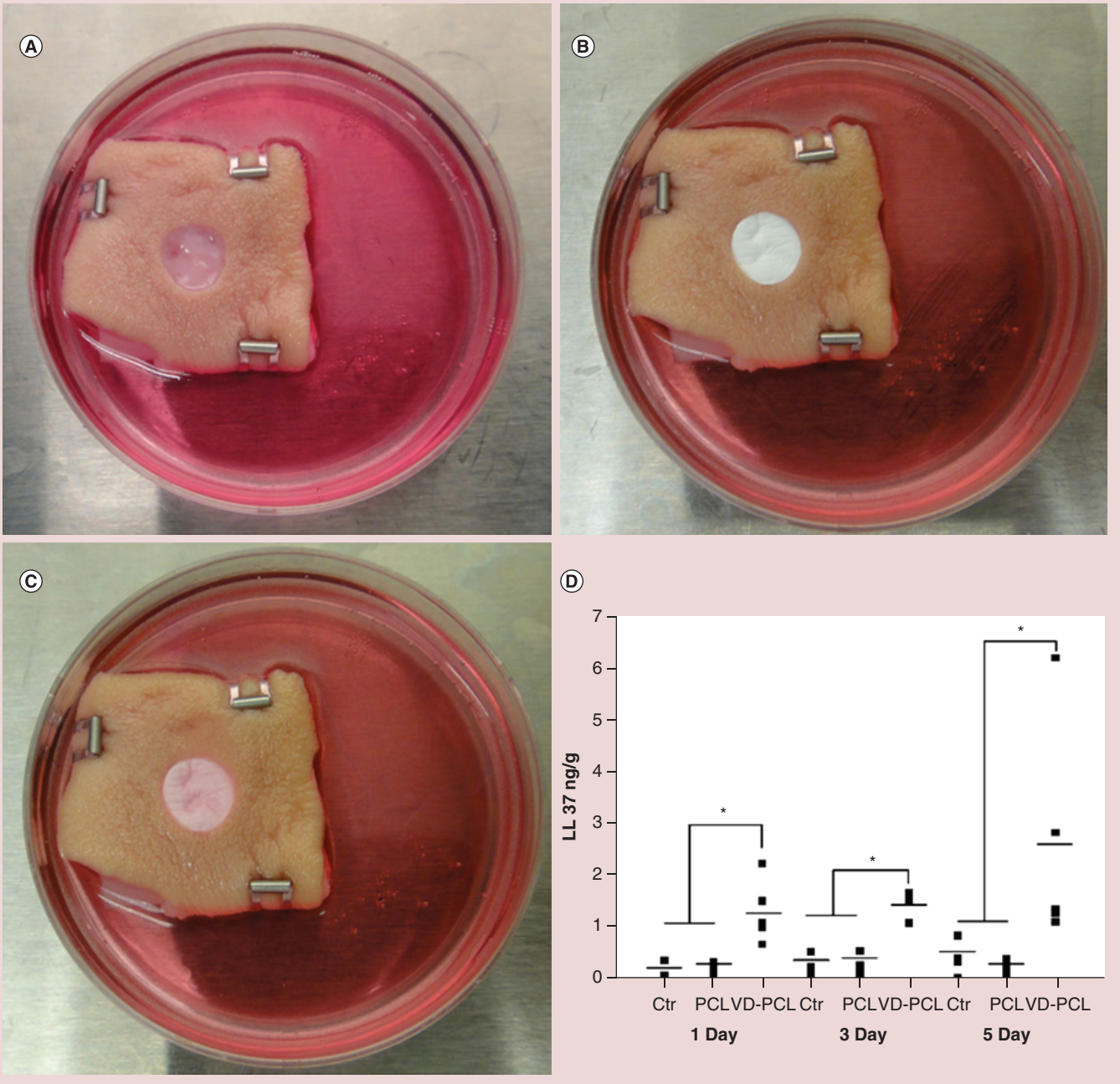

Figure 8. 1,25(OH)$_2$D$_3$-loaded poly(ϵ-caprolactone) nanofibers induce hCAP18/LL37 production in human skin explants. (A) An artificial wound (epidermal and partial dermal layer 1-mm thick) with diameter of 8 mm was created in each skin explant (Ctr: without any treatment). **(B)** Nanofibrous dressings containing either VD-PCL or vehicle (PCL) were placed in the wound. **(C)** Appearance of the skin tissue and nanofiber dressing after 5 days of culture. **(D)** Quantification of hCAP18/LL-37 production by ELISA after treatment for 1, 3 and 5 days. *$p < 0.05$.
Ctr: Control; PCL: Poly(ϵ-caprolactone); VD: 1,25(OH)$_2$D$_3$.

therapeutic anti-infective wound dressings that could improve the host immune response to attack a pathogen on numerous fronts rather than a single front-like traditional antibiotics. In future work, we will test calcipotriol (also known as calcipotriene) and other low calcemic vitamin D analogs that are well tolerated and approved for use in treating psoriasis.

In this study, 2D densely packed nanofiber membranes were used for local delivery of $1,25(OH)_2D_3$ to the wound. To manage fluid transport, wound dressings with tunable porosities and thicknesses are often desired [52]. Traditional nanofiber membranes are usually in a 2D densely packed form [30]. Our recent studies demonstrated a modified gas-foaming technique for fabrication of expanded nanofiber membranes [30,53,54]. In future studies, we will use a modified gas foaming technique without involving an aqueous phase to expand nanofiber membranes in a controlled manner. By this approach, we could control the thickness and porosity of expanded nanofiber membranes while maintaining the bioactivity of encapsulated $1,25(OH)_2D_3$.

In addition to vitamin D_3, lithocholic acid, butyrate, phenylbutyrate, resveratrol, nicotinamide and curcumin induce *CAMP* gene expression in different types of cells. Furthermore, we and others observed synergistic or combinatorial induction of *CAMP* in different cell types by vitamin D_3 given together with resveratrol, pterostilbene, butyrate, phenylbutyrate, trichostatin A, IL-17A, parathyroid hormone, parathyroid hormone-related peptide and entinostat [55–57]. Therefore, we could coencapsulate these immune-modulating compounds in nanofibers for synergistic enhancement of endogenous production of antimicrobial peptides.

To our knowledge, we demonstrate for the first time that grafting PCL nanofibers containing $1,25(OH)_2D_3$ to a wound increases human *CAMP* and hCAP18/LL-37 expression in the skin of transgenic mouse and in human explants. These findings demonstrate that this novel transgenic mouse provides an important model for preclinical studies.

Conclusion

We demonstrated the local delivery of $1,25(OH)_2D_3$ using electrospun nanofibers as carrier. The treatment U937 cells with $1,25(OH)_2D_3$-loaded PCL fibers significantly induced higher cathelicidin protein expression for 5 days compared with free drugs. The skin wounds of human *CAMP* transgenic mice showed a statistically significant 1.5-fold increase in human *CAMP* mRNA expression in the wounds after treatment with $1,25(OH)_2D_3$ containing fibers for 3 days versus the treatment with pristine fibers. Immunohistochemical analysis also showed higher expression of hCAP18/LL-37 in wounds treated with $1,25(OH)_2D_3$-loaded fibers than PCL fibers alone. Additionally, $1,25(OH)_2D_3$-loaded fibers induced higher hCAP18/LL-37 protein expression in human skin explants *ex vivo*. Our findings suggest that local delivery of $1,25(OH)_2D_3$ from nanofibrous dressings could enhance innate immunity by inducing antimicrobial peptide production. This strategy could possibly mitigate selection for multidrug resistance and improve wound healing.

Summary points

- We demonstrated successful encapsulation of $1,25(OH)_2D_3$ in nanofibers using electrospinning.
- The nanofiber-based wound dressings are capable of sustained delivery of $1,25(OH)_2D_3$ over 4 weeks.
- U937 and HaCaT cells treated with $1,25(OH)_2D_3$-loaded poly(ϵ-caprolactone) nanofibers exhibited significant protein (hCAP18/LL37) expression in a sustained manner *in vitro*.
- The skin wounds in human *CAMP* transgenic mice showed a statistically significant 1.5-fold increase in human *CAMP* mRNA expression after 3-day treatment with $1,25(OH)_2D_3$-loaded nanofibers versus pristine fibers only.
- Immunofluorescence analysis of the skin wound tissue in human *CAMP* transgenic mice showed higher expression of hCAP18/LL37 after 3-day treatment with $1,25(OH)_2D_3$-loaded fibers as compared with the pristine fibers.
- $1,25(OH)_2D_3$-loaded nanofibers induced hCAP18/LL37 expression in human skin explants *ex vivo*.

Supplementary data

To view the supplementary data that accompany this paper, please visit the journal website at: www.futuremedicine.com/doi/suppl/10.2217/nnm-2018-0011

Financial & competing interests disclosure

This work was supported by grants from the National Institute of General Medical Science (NIGMS) at the NIH (2P20 GM103480-06 and 1R01GM123081 to J Xie), the Otis Glebe Medical Research Foundation and startup funds from the University of Nebraska Medical Center. The content is solely the responsibility of the authors and does not necessarily represent the official views of the National Institutes of Health. The authors have no other relevant affiliations orfinancial involvement with any organization or entity with a financial interest in or financial conflict with the subject matter or materials discussed in the manuscript apart from those disclosed.

No writing assistance was utilized in the production of this manuscript.

Ethical conduct of research

The authors state that they have obtained appropriate institutional review board approval or have followed the principles outlined in the Declaration of Helsinki for all human or animal experimental investigations. In addition, for investigations involving human subjects, informed consent has been obtained from the participants involved.

References

Papers of special note have been highlighted as: • of interest; •• of considerable interest

1. Mangram AJ, Horan TC, Pearson ML *et al.* Guideline for prevention of surgical site infection. Centers for Disease Control and Prevention (CDC) Hospital Infection Control Practices Advisory Committee. *Am. J. Infect. Control.* 27(2), 97–132 (1999).
2. Magill SS, Edwards JR, Bamberg W *et al.* Multistate point-prevalence survey of health care-associated infections. *N. Engl. J. Med.* 370(13), 1198–1208 (2014).
3. Tsai DM, Caterson EJ. Current preventive measures for health-care associated surgical site infections: a review. *Patient Saf. Surg.* 8(1), 42 (2014).
4. Anderson DJ. Prevention of surgical site infection: beyond SCIP. *AORN J.* 99(2), 315–319 (2014).
5. Yosef I, Manor M, Qimron U. Counteracting selection for antibiotic-resistant bacteria. *Bacteriophage* 6(4), e1096996 (2016).
6. Pendleton JN, Gorman SP, Gilmore BF. Clinical relevance of the ESKAPE pathogens. *Expert Rev. Anti. Infect. Ther.* 11(3), 297–308 (2013).
7. Xie J, Li X, Xia Y. Putting electrospun nanofibers to work for biomedical research. *Macromol. Rapid. Commun.* 29(22), 1775–1792 (2008).
8. Alhnan MA, Basit AW. In-process crystallization of acidic drugs in acrylic microparticle systems: influence of physical factors and drug-polymer interactions. *J. Pharm. Sci.* 100(8), 3284–3293 (2011).
9. Williams GR, Chatterton NP, Nazir T *et al.* Electrospun nanofibers in drug delivery: recent developments and perspectives. *Ther. Del.* 3(4), 515–533 (2012).
10. Xie J, Wang CH. Electrospun micro- and nano-fibers for sustained delivery of paclitaxel to treat C6 glioma *in vitro*. *Pharm. Res.* 23(8), 1817–1826 (2006).
11. Zahedi P, Rezaeian I, Ranaei-Siadat S *et al.* A review on wound dressings with an emphasis on electrospun nanofibrous polymeric bandages. *Polym. Adv. Technol.* 21(2), 77–95 (2010).
12. Kang YO, Yoon IS, Lee SY *et al.* Chitosan-coated poly (vinyl alcohol) nanofibers for wound dressings. *J. Biomed. Mater. Res. B Appl. Biomater.* 92(2), 568–576 (2010).
13. Zimmermann WH, Melnychenko I, Wasmeier G *et al.* Engineered heart tissue grafts improve systolic and diastolic function in infarcted rat hearts. *Nat. Med.* 12(4), 452–458 (2006).
14. Abrigo M, McArthur SL, Kingshott P. Electrospun nanofibers as dressings for chronic wound care: advances, challenges, and future prospects. *Macromol. Biosci.* 14(6), 772–792 (2014).

• **Reviews the electrospun nanofibers as wound dressings for wound care.**

15. Ma ZJ, Ji H, Tan D *et al.* Silver nanoparticles decorated flexible SiO_2 nanofibers with long-term antibacterial effect as reusable wound cover. *Colloids Surf. A Physicochem. Eng. Asp.* 387(1–3), 57–64 (2011).
16. Shalumon KT, Anulekha KH, Nair SV *et al.* Sodium alginate/poly(vinyl alcohol)/nano ZnO composite nanofibers for antibacterial wound dressings. *Int. J. Biol. Macromol.* 49(3), 247–254 (2011).
17. Heunis TDJ, Dicks LMT. Nanofibers offer alternative ways to the treatment of skin infections. *J. Biomed. Biotechnol.* 2010, pii: 510682 (2010).
18. Levy SB. Factors impacting on the problem of antibiotic resistance. *J. Antimicrob. Chemother.* 49(1), 25–30 (2002).
19. Ciornei CD, Egesten A, Bodelsson M. Effects of human cathelicidin antimicrobial peptide LL-37 on lipopolysaccharide-induced nitric oxide release from rat aorta *in vitro*. *Acta Anaesthesiol. Scand.* 47(2), 213–220 (2003).
20. Bjorstad A, Askarieh G, Brown KL *et al.* The host defense peptide LL-37 selectively permeabilizes apoptotic leukocytes. *Antimicrob. Agents Chemother.* 53(3), 1027–1038 (2009).
21. Gombart AF, Borregaard N, Koeffler HP. Human cathelicidin antimicrobial peptide (*CAMP*) gene is a direct target of the vitamin D receptor and is strongly up-regulated in myeloid cells by 1,25-dihydroxyvitamin D_3. *FASEB J.* 19(9), 1067–1077 (2005).

•• **Human *CAMP* gene is strongly upregulated in myeloid cells upon $1,25(OH)_2D_3$ administration.**

22. Gombart AF, Saito T, Koeffler HP. Exaptation of an ancient Alu short interspersed element provides a highly conserved vitamin D-mediated innate immune response in humans and primates. *BMC Genomics* 10, 321 (2009).

•• **Proposes a possible model that explains how the vitamin D_3 pathway may combat infection while minimizing damage to the host by its immune system.**

23. Weber G, Heilborn JD, Chamorro Jimenez CI *et al.* Vitamin D induces the antimicrobial protein hCAP18 in human skin. *J. Invest. Dermatol.* 124(5), 1080–1082 (2005).

• **The expression of *CAMP* is upregulated by calcipotriol in human skin *in vivo*.**

24. Koczulla R, von Degenfeld G, Kupatt C *et al.* An angiogenic role for the human peptide antibiotic LL-37/hCAP-18. *J. Clin. Invest.* 111(11), 1665–1672 (2003).

25. Steinstraesser L, Lam MC, Jacobsen F *et al.* Skin electroporation of a plasmid encoding hCAP-18/LL-37 host defense peptide promotes wound healing. *Mol. Ther.* 22(4), 734–742 (2014).

26. Toniato E, Spinas E, Saggini A *et al.* Immunomodulatory effects of vitamin D on skin inflammation. *J. Biol. Regul. Homeost. Agents* 29(3), 563–567 (2015).

27. Jiang J, Chen G, Shuler FD *et al.* Local sustained delivery of 25-hydroxyvitamin D_3 for production of antimicrobial peptides. *Pharm. Res.* 32(9), 2851–2862 (2015).

•• **This work demonstrates the sustained delivery of 25-hydroxyvitamin D_3 is capable of inducing antimicrobial peptides in monocytes and keratinocytes.**

28. Chen S, Ge L, Gombart AF *et al.* Nanofiber-based sutures induce endogenous antimicrobial peptide. *Nanomedicine* 12(21), 2597–2609 (2017).

29. Xie J, Tan R, Wang CH. Biodegradable microparticles and fiber fabrics for sustained delivery of cisplatin to treat C6 glioma *in vitro*. *J. Biomed. Mater. Res. Part A* 85(4), 897–908 (2008).

30. Jiang J, Carlson MA, Teusink MJ *et al.* Expanding two-dimensional electrospun nanofiber membranes in the third dimension by a modified gas-foaming technique. *ACS Biomater. Sci. & Eng.* 1(10), 991–1001 (2015).

31. Xie J, Zhong S, Ma B *et al.* Controlled biomineralization of electrospun (poly-caprolactone) fibers to enhance their mechanical properties. *Acta Biomater*. 9, 5698–5707 (2013).

32. Liang X, Bhattacharya S, Bajaj G *et al.* Delayed cutaneous wound healing and aberrant expression of hair follicle stem cell markers in mice selectively lacking ctip2 in epidermis. *PLoS ONE* 7(2), e29999 (2012).

33. Ganguli-Indra G. Chapter 12 Protocol for cutaneous wound healing assay in a murine model. In: *Stem Cells and Tissue Repair: Methods and Protocols, Methods in Molecular Biology (Volume 1210)*. Kioussi C (Ed.). Humana Press, NY, USA, 151–159 (2014).

34. Campbell Y. *The effect of dietary compounds on human cathelicidin antimicrobial peptide gene expression mediated through farnesoid X receptor and its potential role in gastrointestinal health [Doctoral dissertation]*. Retrieved from Scholars Archive@OSU, Corvallis, OR, USA (2013).

35. Guo C, Rosoha E, Lowry MB *et al.* Curcumin induces human cathelicidin antimicrobial peptide gene expression through a vitamin D receptor-independent pathway. *J. Nutr. Biochem.* 24(5), 754–759 (2013).

36. Woodruff MA, Hutmacher DW. The return of a forgotten polymer-polycaprolactone in the 21st century. *Prog. Polym. Sci.* 35(10), 1217–1256 (2010).

37. Gurtner GC, Werner S, Barrandon Y *et al.* Wound repair and regeneration. *Nature* 453(7193), 314–321 (2010).

38. Werner S, Grose R. Regulation of wound healing by growth factors and cytokines. *Physiol. Rev.* 83(3), 835–870 (2003).

39. Mangelsdorf DJ, Thummel C, Beato M *et al.* The nuclear receptor superfamily: the second decade. *Cell* 83(6), 835–839 (1995).

40. Christakos S, Raval-Pandya M, Wernyj RP *et al.* Genomic mechanisms involved in the pleiotropic actions of 1,25-dihydroxyvitamin D_3. *Biochem. J.* 316(Pt 2), 361–371 (1996).

41. Rid R, Wagner M, Maier CJ *et al.* Deciphering the calcitriol-induced transcriptomic response in keratinocytes: presentation of novel target genes. *J. Mol. Endocrinol.* 50(2), 131–149 (2013).

42. Wang TT, Nestel FP, Bourdeau V *et al.* Cutting edge: 1,25-dihydroxyvitamin D_3 is a direct inducer of antimicrobial peptide gene expression. *J. Immunol.* 173(5), 2909–2912 (2004).

•• **Shows that $1,25(OH)_2D_3$ is a direct regulator of antimicrobial innate immune responses.**

43. Lowry MB, Guo C, Borregaard N *et al.* Regulation of the human cathelicidin antimicrobial peptide gene by 1,25-dihydroxyvitamin D_3 in primary immune cells. *J. Steroid Biochem. Mol. Biol.* 143, 183–191 (2014).

44. Heilborn JD, Nilsson MF, Kratz G *et al.* The cathelicidin anti-microbial peptide LL-37 is involved in re-epithelialization of human skin wounds and is lacking in chronic ulcer epithelium. *J. Invest. Dermatol.* 120(3), 379–389 (2003).

45. Dorschner RA, Pestonjamasp VK, Tamakuwala S *et al.* Cutaneous injury induces the release of cathelicidin anti-microbial peptides active against group A *Streptococcus*. *J. Invest. Dermatol.* 117(1), 91–97 (2001).

46. Frohm Nilsson M, Sandstedt B, Sørensen O *et al.* The human cationic antimicrobial protein (hCAP18), a peptide antibiotic, is widely expressed in human squamous epithelia and colocalizes with interleukin-6. *Infect. Immun.* 67(5), 2561–2566 (1999).

47. Schauber J, Dorschner RA, Coda AB *et al.* Injury enhances TLR2 function and antimicrobial peptide expression through a vitamin D-dependent mechanism. *J. Clin. Invest.* 117(3), 803–811 (2007).

48. Turner J, Cho Y, Dinh NN *et al.* Activities of LL-37, a cathelin-associated antimicrobial peptide of human neutrophils. *Antimicrob. Agents Chemother.* 42(9), 2206–2214 (1998).

49. Saiman L, Tabibi S, Starner TD *et al.* Cathelicidin peptides inhibit multiply antibiotic-resistant pathogens from patients with cystic fibrosis. *Antimicrob. Agents Chemother.* 45(10), 2838–2844 (2001).

50. Nizet V, Ohtake T, Lauth X *et al.* Innate antimicrobial peptide protects the skin from invasive bacterial infection. *Nature* 414(6862), 54–457 (2001).

●● **Cathelicidins are an important native component of innate host defense in mice and provide protection against necrotic skin infection caused by Group A *Streptococcus*.**

51. Nakatsuji T, Chen TH, Two AM *et al.* Staphylococcus aureus exploits epidermal barrier defects in atopic dermatitis to trigger cytokine expression. *J. Invest. Dermatol.* 136(11), 2192–2200 (2016).

52. Doillon CJ, Whyne CF, Brandwein S *et al.* Collagen-based wound dressings: control of the pore structure and morphology. *J. Biomed. Mater. Res. A* 20(8), 1219–1228 (1986).

53. Jiang J, Li Z, Wang H *et al.* Expanded 3D nanofiber scaffolds: cell penetration, neovascularization, and host response. *Adv. Healthc. Mater.* 5(23), 2993–3003 (2016).

54. Jiang J, Chen S, Wang H *et al.* CO_2-expanded nanofiber scaffolds maintain activity of encapsulated bioactive materials and promote cellular infiltration and positive host response. *Acta Biomater.* 68, 237–248 (2018).

●● **Demonstrates the expansion of nanofiber mats with controlled thickness through depressurization of subcritical CO_2 fluid.**

55. Peric M, Koglin S, Kim SM *et al.* IL-17A enhances vitamin D_3-induced expression of cathelicidin antimicrobial peptide in human keratinocytes. *J. Immunol.* 181(12), 8504–8512 (2008).

56. Muehleisen B, Bikle DD, Aguilera C *et al.* PTH/PTHrP and vitamin D control antimicrobial peptide expression and susceptibility to bacterial skin infection. *Sci. Transl. Med.* 4(135), 135ra66 (2012).

57. Ottosson H, Nylen F, Sarker P *et al.* Potent inducers of endogenous antimicrobial peptides for host direct therapy of infections. *Sci. Rep.* 6, 36692 (2016).